ANESTHESIOLOGY

Comparison of Neonatal and Adult Fibrin Clot Properties between Porcine and Human Plasma

Kimberly A. Nellenbach, B.S., Seema Nandi, B.S., Alexander Kyu, Supriya Sivadanam, B.S., Nina A. Guzzetta, M.D., F.A.A.P., Ashley C. Brown, Ph.D.

ANESTHESIOLOGY 2020; 132:1091–101

EDITOR'S PERSPECTIVE

What We Already Know about This Topic

- Neonatal fibrinogen exists in a fetal form until maturation and is structurally and functionally distinct from adult fibrinogen
- Replacement of neonatal fibrinogen with adult fibrinogen after cardiopulmonary bypass may lead to inconsistent efficacy in treating postcardiopulmonary bypass bleeding
- The hemostatic system of pigs is similar to that of humans

What This Article Tells Us That Is New

- Fibrinogen concentration and functionality in plasma collected from piglets paralleled those observed in plasma collected from human neonates
- Fibrin network structure was highly aligned in both neonatal species and highly branched in adults of both species
- Fibrin network stiffness and degradation patterns in both neonatal species were substantially similar as they were in adults of both species
- The *ex vivo* addition of several procoagulant therapies augmented fibrin network properties of diluted piglet plasma

ABSTRACT

Background: Recent studies suggest that adult-specific treatment options for fibrinogen replacement during bleeding may be less effective in neonates. This is likely due to structural and functional differences found in the fibrin network between adults and neonates. In this investigation, the authors performed a comparative laboratory-based study between immature and adult human and porcine plasma samples in order to determine if piglets are an appropriate animal model of neonatal coagulopathy.

Methods: Adult and neonatal human and porcine plasma samples were collected from the Children's Hospital of Atlanta and North Carolina State University College of Veterinary Medicine, respectively. Clots were formed for analysis and fibrinogen concentration was quantified. Structure was examined through confocal microscopy and cryogenic scanning electron microscopy. Function was assessed through atomic force microscopy nanoindentation and clotting and fibrinolysis assays. Lastly, novel hemostatic therapies were applied to neonatal porcine samples to simulate treatment.

Results: All sample groups had similar plasma fibrinogen concentrations. Neonatal porcine and human plasma clots were less branched with lower fiber densities than the dense and highly branched networks seen in adult human and porcine clots. Neonatal porcine and human clots had faster degradation rates and lower clot stiffness values than adult clots (stiffness [mmHg] mean ± SD: neonatal human, 12.15 ± 1.35 mmHg *vs.* adult human, 32.25 ± 7.13 mmHg; $P = 0.016$; neonatal pig, 10.5 ± 8.25 mmHg *vs.* adult pigs, 32.55 ± 7.20 mmHg; $P = 0.015$). The addition of hemostatic therapies to neonatal porcine samples enhanced clot formation.

Conclusions: The authors identified similar age-related patterns in structure, mechanical, and degradation properties between adults and neonates in porcine and human samples. These findings suggest that piglets are an appropriate preclinical model of neonatal coagulopathy. The authors also show the feasibility of *in vitro* model application through analysis of novel hemostatic therapies as applied to dilute neonatal porcine plasma.

(ANESTHESIOLOGY 2020; 132:1091–101)

The coagulation system is immature at birth and matures throughout the first year of life.[1–3] Physiologically healthy newborns show excellent hemostasis, but when compromised (*e.g.,* critically ill neonates undergoing major surgery with cardiopulmonary bypass [CPB] or extracorporeal membrane oxygenation), their neonatal hemostatic immaturity can have critical clinical implications,[2,4] and is a contributory factor to serious postoperative bleeding. The current standard-of-care treatment for bleeding in neonates is the transfusion of adult blood products including packed erythrocytes, platelets, cryoprecipitate (fibrinogen component), and fresh frozen plasma.[4–6] However, this treatment has inconsistent efficacy and the use of allogenic blood products is associated with multiple infectious and noninfectious risks.[5] Additionally, our recent studies demonstrate

Supplemental Digital Content is available for this article. Direct URL citations appear in the printed text and are available in both the HTML and PDF versions of this article. Links to the digital files are provided in the HTML text of this article on the Journal's Web site (www.anesthesiology.org). Part of this work has been presented at the American Heart Association's Vascular Discovery 2019 Scientific Sessions in Boston, Massachusetts, May 15, 2019.

Submitted for publication July 8, 2019. Accepted for publication January 3, 2020. Published online first on January 30, 2020. From the Joint Department of Biomedical Engineering, North Carolina State University and The University of North Carolina at Chapel Hill, Raleigh, North Carolina (K.A.N., S.N., A.K., S.S., A.C.B.); the Comparative Medicine Institute, North Carolina State University, Raleigh, North Carolina (K.A.N., A.C.B.); and the Department of Anesthesiology, Emory University School of Medicine and Children's Healthcare of Atlanta, Atlanta, Georgia (N.A.G.).

 Anesthesiology 2020; 132:1091–101. DOI: 10.1097/ALN.0000000000003165

<zdoi;. DOI: 10.1097/ALN.0000000000003165>

that one of the essential clotting proteins, fibrinogen, is structurally and functionally distinct between neonates and adults. Moreover, when mixed together to simulate transfusion of cryoprecipitate (adult fibrinogen component), the resulting fibrin networks are structurally and functionally distinct compared to those formed solely from native neonatal fibrinogen.[7]

Recent investigations in developmental hemostasis indicate that neonatal fibrinogen exists in a fetal form until maturation and that its replacement with adult fibrinogen after CPB may lead to inconsistent efficacy in treating post-CPB bleeding.[7–9] Developing neonatal specific treatment strategies to mitigate bleeding, especially during or after major surgery, could potentially improve outcomes in this challenging patient population. Unfortunately, there has been no validation of the observed differences in neonatal *versus* adult fibrin structure in animal models. Establishing a validated animal model would facilitate the preclinical analysis of neonatal specific hemostatic therapies prior to the implementation of clinical trials.

Here, we performed a comparative study between neonatal and adult human and porcine plasma samples to determine if piglets accurately reflect the maturation of human fibrinogen. Pigs represent an appealing model to use in translational medicine due to their anatomical and physiologic similarities to humans, particularly in regard to the hemostatic system.[10–13] Thus, we hypothesize that pigs possess age-related differences in fibrinogen that parallel those identified in humans.[14] The primary objective of this study was to validate the fibrin network in piglets as an appropriate *in vitro* animal model for that of human neonates. We accomplish this by characterizing fibrin network parameters formed from plasma collected from neonatal and adult humans and pigs. Our second objective was to analyze the *in vitro* effect of several novel and commercially relevant procoagulant therapies on the fibrin network properties of neonatal porcine samples. We utilized a model of post-CPB dilutional coagulopathy because procoagulant therapies are currently being used off-label as rescue agents to control bleeding after CPB in neonates when conventional blood transfusions fail.[5,15,16] Also, our previous studies demonstrate that the *ex vivo* addition of procoagulant therapies to post-CPB plasma from human neonates enhances fibrin clot properties.[17–20] We hypothesize that the *in vitro* addition of these hemostatic therapies to neonatal porcine samples will similarly augment plasma fibrin clot properties. If confirmed, piglets could serve as a suitable and much needed preclinical model for evaluating neonatal specific hemostatic therapies.

Materials and Methods

Human Plasma Collection

After Institutional Review Board approval and parental informed written consent, blood samples were collected from 10 human neonates (aged less than 30 days) undergoing corrective and palliative cardiac surgery with CPB at the Children's Hospital of Atlanta (Atlanta, Georgia). All samples were collected from an arterial line placed after the induction of anesthesia and before surgical incision and CPB. Samples were centrifuged immediately to yield platelet-poor plasma and stored at −80°C until use. All patient samples were deidentified before sample transfer to North Carolina State University (Raleigh, North Carolina). Pooled adult human platelet-poor plasma was obtained from the New York Blood Center (New York, New York).

Porcine Plasma Collection

Blood was collected from eight 1-yr-old female Yorkshire pigs and eight 8-week-old Yorkshire piglets before planned surgical procedures at North Carolina State University's School of Veterinary Medicine (Raleigh, North Carolina, USA) through the tissue sharing program. Porcine ages and sample size were selected in order to minimize animal use. For this study, we utilized samples from pigs that were readily available in sufficient numbers. All samples were collected *via* jugular venous puncture after the induction of anesthesia and before surgical incision. Samples were centrifuged immediately to obtain platelet-poor plasma and stored at −80°C until use.

Quantification and Isolation of Fibrinogen from Platelet Poor Plasma

Quantification of fibrinogen concentration was achieved *via* enzyme linked immunosorbent assays ([ELISA] Abcam, USA) with human and porcine protein quantification kits. Isolated fibrinogen was utilized for clottability assays. Fibrinogen was purified from plasma *via* an ethanol precipitation reaction. Briefly, ethanol (70% volume) was added to 4°C plasma in a 4:1 ratio (plasma:ethanol) and cooled on ice for 20 min. The solution was then centrifuged for 15 min at 4°C. The supernatant plasma was removed and the resulting pellet was heated in a 37°C water bath. A buffer consisting of 20 mM sodium citrate was added until the pellet was fully dissolved. Protein concentration was determined *via* absorbance readings at 280 nm using a Nanodrop Microvolume UV-Vis Spectrophotometer (ThermoFisher Scientific, USA).

Analysis of Fibrinogen Clottability

Percentage of total fibrinogen clottability was determined by a protein quantification-based assay which measures the protein content in the clot liquor (soluble portion of clot sample) that remains after polymerization. Clots totaling 50 μl were formed with purified fibrinogen at a concentration of 2.5 mg/ml, HEPES buffer (5 mM calcium; 7.4 pH) and were polymerized with the initiation of 0.5 U/ml thrombin. Before and after a 1-h polymerization period, 5-μl aliquots were taken and quantified *via* NanoOrange Protein

Quantification Kit (Invitrogen, USA). Alternately, 50-μl plasma clots were formed with 0.5 U/ml thrombin, and quantification was conducted *via* ELISA for pig or human fibrinogen (Abcam, USA). Percent of clottable fibrinogen was determined as: ([initial soluble protein – soluble protein in clot liquor] / initial soluble protein) × 100.[21]

Analysis of Clot Architecture

Confocal microscopy was utilized to examine clot structure from neonatal and adult human and porcine plasma samples. Clots consisting of 90% plasma by volume were polymerized with 0.1, 0.25, or 0.5 U/ml of human thrombin (Enzyme Research Labs, USA), and 10 μg/ml of Alexa Fluor 488–labeled fibrinogen for visualization. Clots were formed between a glass slide and coverslip, and allowed to polymerize for 2 h before imaging. A Zeiss Laser Scanning Microscope (LSM 710; Zeiss Inc., USA) was utilized for imaging at a magnification of 63× and a minimum of three random 5.06-μm z-stacks were acquired per clot. ImageJ software was used to create three-dimensional projections from z-stacks. Clot fiber density was determined from the ratio of black (fiber) over white (background) pixels in each image. Fibrin clot alignment was quantified with a custom MATLAB algorithm previously utilized in Brown *et al.*[7,22] An alignment index was determined from the fraction of fibers aligned within ± 20° of a preferred fiber alignment normalized to random distribution of oriented fibers. A greater alignment index corresponds to a higher percentage of fibers aligned near the preferred fiber alignment. Alignment index values ranged from 1.0 to 4.55. Alignment analysis was conducted for each image in the z-stack and averaged together. Clot structure in porcine samples was additionally assessed with cryogenic scanning electron microscopy to examine three-dimensional clot architecture. Again, 50-μl plasma clots were formed with 0.5 U/ml thrombin and allowed to polymerize for 2 h before imaging. Clots were rapidly frozen in subcooled liquid nitrogen and imaged at 2,500×. Three clots were imaged per group and three random images were taken per clot.

Analysis of Clot Stiffness

Clot mechanical properties were examined using atomic force microscopy (Asylum MFP3D-Bio; Asylum Research, USA) operated in force contact mode to obtain stiffness values. Plasma clots formed with 0.5 U/ml human thrombin were polymerized directly on a glass slide 1.5 h before force measurements. Standard silicon nitride cantilevers with a particle diameter of 1.98 μm (Nanoandmore, USA) were utilized. Force maps of 20 μm × 20 μm dimensions were collected on each clot and fit with a Hertz model to obtain the elastic modulus. A minimum of two random force maps were generated per clot with the average elastic modulus reported.

Analysis of Clot Degradation

Fibrinolysis was assessed for neonatal and adult human and porcine samples. A custom microfluidics based assay adapted from Brown *et al.* was utilized to analyze degradation rates for all sample groups.[17,18] A polydimethylsiloxane (Dow Corning, USA) device consisting of a clot reservoir with a perpendicular lying channel was constructed *via* casting in an acrylic mold. After curing for 24 h, the device was plasma treated and bonded to a glass slide to create a sealed channel. Clots were formed from plasma and 10% Alexa Fluor 488–labeled adult fibrinogen was added for visualization. Polymerization was initiated with the addition of 0.5 U/ml thrombin, and 25 μl of the clot solution was immediately injected into the clot reservoir. After polymerizing for 2 h, the device was mounted on an EVOS FL Auto microscope (Life Technologies, USA) for imaging. A plasmin solution (0.01 mg/ml plasmin in HEPES buffer) (Human Plasmin; Enzyme Research Laboratories, USA) was injected into a channel inlet, and the clot was imaged every 10 min for 12 h. ImageJ (National Institutes of Health, USA) was used to determine rate of clot degradation by comparing the first and final images and measuring distance along a perpendicular line to the clot boundary. Clot degradation rates were expressed as the distance the clot boundary traveled divided by 12 h.

Analysis of Procoagulants in a Hemodilution Model of Coagulopathy

To mimic the reduction of clotting factors seen after CPB, porcine plasma was diluted for all subsequent assays. Initial fibrinogen levels of 8-week-old porcine plasma were determined *via* ELISA (Pig Fibrinogen ELISA; Abcam, USA). For all structural and functional assays, plasma was diluted to a final concentration of 1.5 mg/ml to match the fibrinogen concentration in human neonates post-CPB observed in our previous studies.[7] The following procoagulants were added to the dilute neonatal plasma to simulate treatment after CPB: recombinant activated factor VII (Novo Nordisk Inc., USA), factor eight inhibitor bypassing activity (Shire US Inc., USA), RiaSTAP Fibrinogen Concentrate (CSL Behring, Germany), and novel synthetic platelet-like particles developed by our group. We chose the aforementioned therapies because factor VIIa, factor eight inhibitor bypassing activity, and RiaSTAP have been used off-label as rescue agents to control bleeding after CPB in neonates when the standard of care fails.[5,15,16] Additionally, factor eight inhibitor bypassing activity, a prothrombin complex concentrate, was utilized in this study because of its use at our clinical institution. However, it should be noted that Kcentra is an additional prothrombin complex concentrate that is also used clinically. The synthetic platelet-like particles utilized for these studies have previously been shown to enhance human neonatal fibrin clot properties *in vitro*.[17] Diluted porcine plasma was used to form 50-μl clots with

0.5 U/ml thrombin in the presence of 0.05 mg/ml factor VIIa, 0.3 U/ml factor eight inhibitor bypassing activity, 0.89 mg/ml RiaSTAP, or 0.5 mg/ml platelet-like particles. Factor VIIa, RiaSTAP, and factor eight inhibitor bypassing activity concentrations were chosen to reflect a clinically utilized dose, while the platelet-like particle concentration was chosen based off of optimized experiments previously conducted by our group.[19] Synthetic platelet-like particles were synthesized and characterized as previously described by covalently coupling highly deformable ultralow crosslinked microgels to a fibrin-specific antibody.[17] Ultralow crosslinked poly(N-isopropylacrylamide-co-acrylic acid) microgels were synthesized *via* a precipitation polymerization reaction and characterized *via* atomic force microscopy dry imaging to determine particle deformability (Supplemental Digital Content 1, http://links.lww.com/ALN/C237). Platelet-like particles were created by covalently coupling microgels to a sheep anti-human fibrin fragment E polyclonal IgG antibody using N-(3-Dimethylaminopropyl)-*N*'-ethylcarbodiimide hydrochloride/N-hydroxysuccinimide chemistry. Particles were purified *via* dialysis for 72 h, lyophilized, and resuspended at 10 mg/ml. For analysis of clot structure in the presence and absence of hemostatic therapies, confocal microscopy was utilized as previously described. To examine clottability of diluted plasma with and without the addition of procoagulant agents, 50-μl clots were formed and protein quantified before and after polymerization. Fibrinogen was quantified *via* ELISA (Pig Fibrinogen ELISA; Abcam, USA) and clottability was calculated as previously described.

Statistical Analysis

All statistical analyses were performed with a repeated measures one-way ANOVA test using GraphPad Prism Software (USA) with a Tukey *post hoc* analysis with a 95% CI. Analysis was performed between sample groups. Statistical significance was achieved for $P < 0.05$. No *a priori* statistical power calculation was conducted. Data is defined as interval and is presented as average ± SD. Outlier tests were performed on all datasets before graph creation and statistical analysis. No outliers were identified. There were no missing data.

Results

Quantification of Plasma Fibrinogen Levels

Fibrinogen concentrations were quantified across age groups and species (fig. 1). We observed similar values of fibrinogen across species and age groups that is consistent with previous studies (neonatal humans, 246 ± 90 mg/dl; neonatal pigs, 295 ± 89 mg/dl; adult humans, 265 ± 116 mg/dl; adult pigs, 346 ± 59 mg/dl; neonatal humans *vs.* adult humans, $P = 0.993$, neonatal pigs *vs.* adult pigs: $P = 0.898$, neonatal human *vs.* neonatal pigs: $P = 0.909$; adult human *vs.* adult pigs, $P = 0.705$). Additionally, porcine fibrinogen concentrations were within normal human ranges of 200 to 450mg/dl.[23]

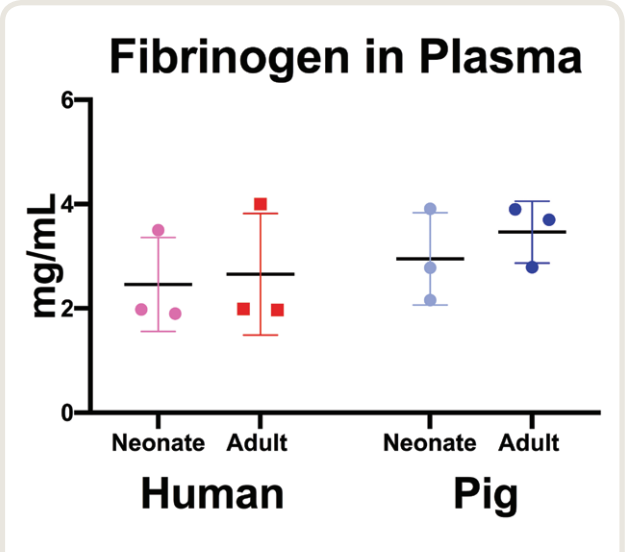

Fig. 1. Quantification of fibrinogen levels in platelet poor plasma. Fibrinogen was quantified *via* enzyme linked immunosorbent assays across species and age ranges. Average fibrinogen concentrations ± SD is shown. N = 3.

Analysis of Fibrinogen Clottability

To compare functional ability of fibrinogen across species and age groups, clottability of the purified protein was quantified (fig. 2). We demonstrate that neonatal samples had statistically significant lower clottability across species

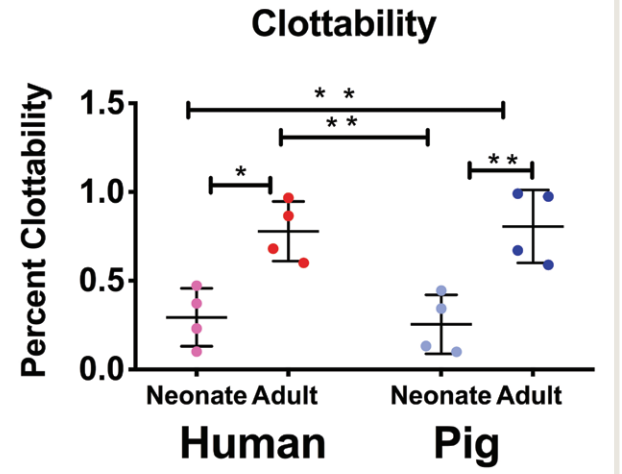

Fig. 2. Quantification of isolated fibrinogen clottability across species. Clottability of purified fibrinogen was determined *via* NanoOrange Protein Quantification Kit. Average clottability ± SD is reported. N = 4 *$P < 0.05$, **$P < 0.01$.

compared to their adult counterparts (neonatal humans, 29 ± 16%; neonatal pigs, 25 ± 17%; adult humans, 78 ± 17%; adult pigs, 81 ± 21%; neonatal humans *vs.* adult humans, $P = 0.010$; neonatal pigs *vs.* adult pigs, $P = 0.004$). Neonatal humans and pigs had similar clottability ($P = 0.989$) values, as did adult samples ($P = 0.995$).

Analysis of Clot Architecture

We first examined and contrasted the fibrin clot structure with confocal microscopy between adult and neonatal porcine samples as a function of thrombin concentration (fig. 3). In general, adult porcine clots were denser and more heavily branched with increasing fiber density with increasing thrombin concentration. Fiber density is calculated as the ratio of black pixels (fibers) over white pixels (blank space), therefore this measurement is unitless. Conversely, neonatal porcine fibrin clots were more aligned with a lower fiber density compared to adults (alignment index values: neonatal pigs: 0.1, 0.25, 0.5 U/ml thrombin, 1.12 ± 0.05, 1.18 ± 0.08, 1.15 ± 0.09; adult pigs: 0.1, 0.25, 0.5 U/ml thrombin, 1.07 ± 0.006, 1.08 ± 0.05, 1.07 ± 0.07; 0.1 U/ml thrombin: neonatal pigs *vs.* adult pigs, $P = 0.814$; 0.25 U/ml thrombin: neonatal pigs *vs.* adult pigs, $P = 0.063$; 0.5 U/ml thrombin: neonatal pigs *vs.* adult pigs, $P = 0.196$; fiber density: neonatal pigs: 0.1, 0.25, 0.5 U/ml thrombin, 0.23± 0.19, 0.25± 0.29, 0.54 ± 0.16; adult pigs: 0.1, 0.25, 0.5 U/ml thrombin, 0.56 ± 0.21, 1.19 ± 0.72, 1.27 ± 0.36; 0.1 U/ml thrombin: neonatal pigs *vs.* adult pigs, $P = 0.801$; 0.25 U/ml thrombin: neonatal pigs *vs.* adult pigs, $P = 0.026$; 0.5 U/ml thrombin: neonatal pigs *vs.* adult pigs, $P = 0.118$). For all subsequent structural analyses, a thrombin concentration of 0.5 U/ml was utilized. We also examined and contrasted fibrin clot structure with cryogenic scanning electron microscopy between neonatal and adult porcine samples (Supplemental Digital Content 2, http://links.lww.com/ALN/C238). Three-dimensional structure reflected similar structural patterns identified *via* confocal microscopy with neonatal porcine samples more highly aligned compared to the densely branched network in adult porcine clots. However, because the freezing technique required for cryogenic scanning electron microscopy may impact clot porosity, it was utilized as a secondary method of image analysis and did not include quantitative analysis. Next, we utilized confocal microscopy to examine fibrin clot architecture across species (fig. 4). In general, age-related structural relationships were consistent across species. Neonatal porcine and human clots exhibited minimally branched, aligned, sheet-like fibrin matrices with significantly lower fiber densities than the adult groups (neonatal humans, 0.61 ± 0.28; neonatal pigs, 0.54 ± 0.16; adult humans, 1.41 ± 0.5; adult pigs, 1.27 ± 0.36 black/white pixels; neonatal humans *vs.* adult humans, $P = 0.043$; neonatal pigs *vs.* adult pigs, $P = 0.035$; neonatal human

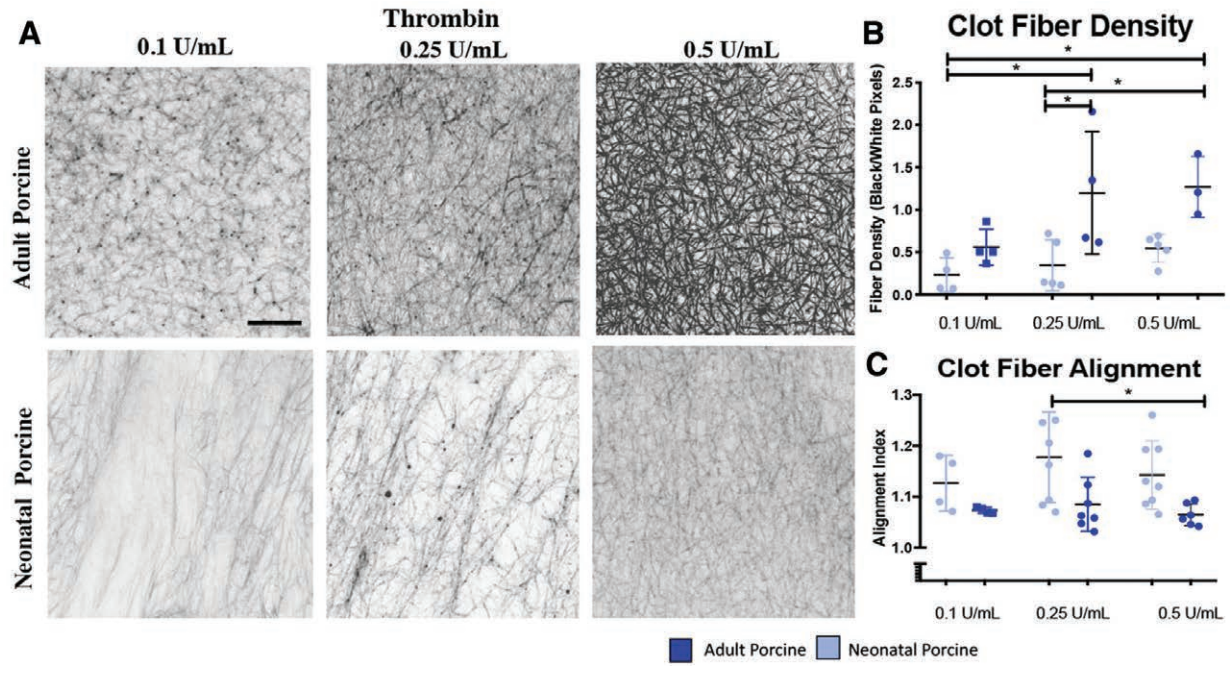

Fig. 3. Confocal microscopy analysis of structure of adult and neonatal porcine clots formed with increasing thrombin (*A*). Average clot fiber alignment (*B*) and fiber density (*C*) ± SD are shown. 0.1 U/ml thrombin: neonatal pigs, N = 4; adult pigs, N = 4; 0.25 U/ml thrombin: neonatal pigs, N = 8; adult pigs, N = 7; 1.0 U/ml thrombin: neonatal pigs, N = 8; adult pigs, N = 6. *$P < 0.05$.

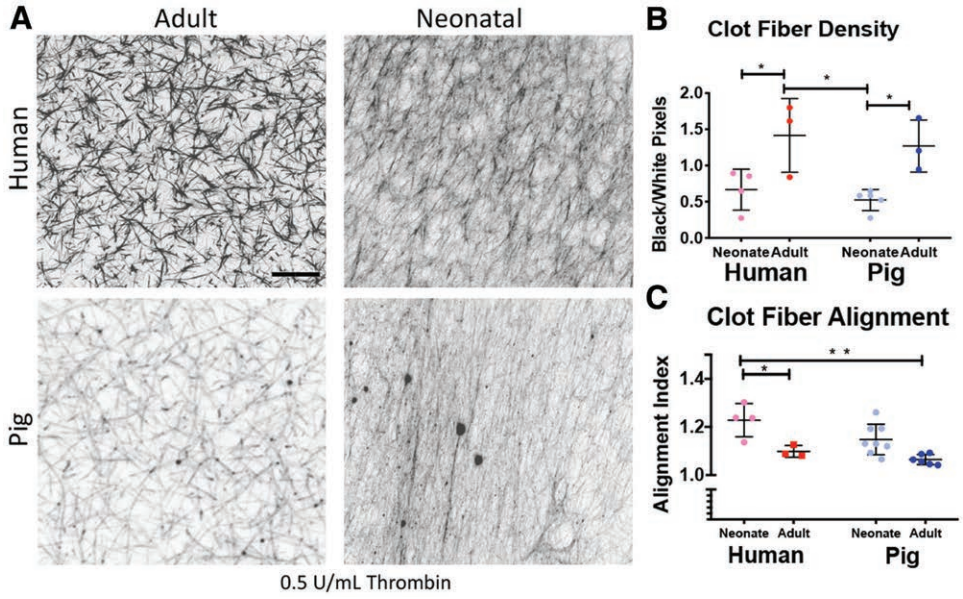

Fig. 4. Confocal microscopy analysis of structure of adult and neonatal human and porcine clots formed with 0.5 U/ml thrombin (*A*). Average clot fiber alignment (*B*) and fiber density (*C*) ± SD is shown. Alignment: neonatal humans, N = 4; adult humans, N = 3; neonatal pigs, N = 8; adult pigs, N = 6. Fiber Density: neonatal humans, N = 4; adult humans, N = 3; neonatal pigs, N = 5; adult pigs, N = 3. **P* < 0.05, ***P* < 0.01.

vs. neonatal pigs, $P = 0.903$; adult human *vs.* adult pigs, $P = 0.938$). Neonatal human and porcine samples resulted in higher clot fiber alignment values than adult humans or pigs (neonatal humans, 1.22 ± 0.09; neonatal pigs, 1.14 ± 0.07; adult humans, 1.09 ± 0.02; adult pigs, 1.07 ± 0.02; neonatal humans *vs.* adult humans, $P = 0.021$; neonatal pigs *vs.* adult pigs, $P = 0.051$; neonatal human *vs.* neonatal pigs, $P = 0.092$; adult human *vs.* adult pigs, $P = 0.795$).

Analysis of Clot Stiffness

Fibrin clot mechanical properties were evaluated *via* atomic force microscopy nanoindentation. Force maps were generated (Supplemental Digital Content 3, http://links.lww.com/ALN/C239); average stiffness values are shown in figure 5. We observed statistically significant lower clot stiffness values in neonatal human plasma clots compared to adults. These tendencies were mirrored in porcine samples (neonatal humans, 12.15 ± 1.35 mmHg [1.60 ± 0.18 kPa]; neonatal pigs, 10.50 ± 8.25 mmHg [1.40 ± 1.1 kPa]; adult humans, 32.25 ± 7.13 mmHg [4.3 ± 0.95 kPa]; adult pigs, 32.55 ± 7.20 mmHg [4.3 ± 0.96 kPa]; neonatal humans *vs.* adult humans, $P = 0.016$; neonatal pigs *vs.* adult pigs, $P = 0.015$; neonatal human *vs.* neonatal pigs, $P > 0.999$; adult human *vs.* adult pigs, $P > 0.999$).

Analysis of Clot Degradation

A custom microfluidics assay was utilized to determine plasma clot degradation rates (fig. 6).[7] Clots formed from neonatal human and pig plasma samples had significantly faster rates of degradation compared to adult human and pig groups (neonatal humans, 24.9 ± 4.9 μm/h; neonatal pigs, 32.6 ± 5.2 μm/h; adult humans, 13.9 ± 3.1 μm/h; adult pigs, 12.4 ± 4.1 μm/h; neonatal humans *vs.* adult humans, $P = 0.048$; neonatal pigs *vs.* adult pigs, $P < 0.0001$; neonatal human *vs.* neonatal pigs, $P = 0.140$; adult human *vs.* adult pigs, $P = 0.969$).

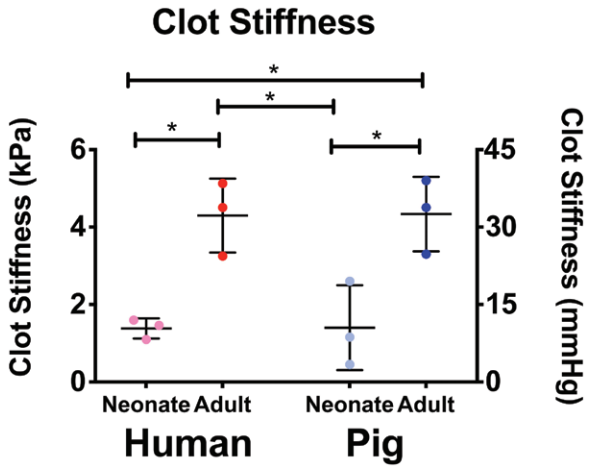

Fig. 5. Atomic force microscopy analysis of plasma clot stiffness across species. Mean stiffness ± SD is shown. N = 3; **P* < 0.05.

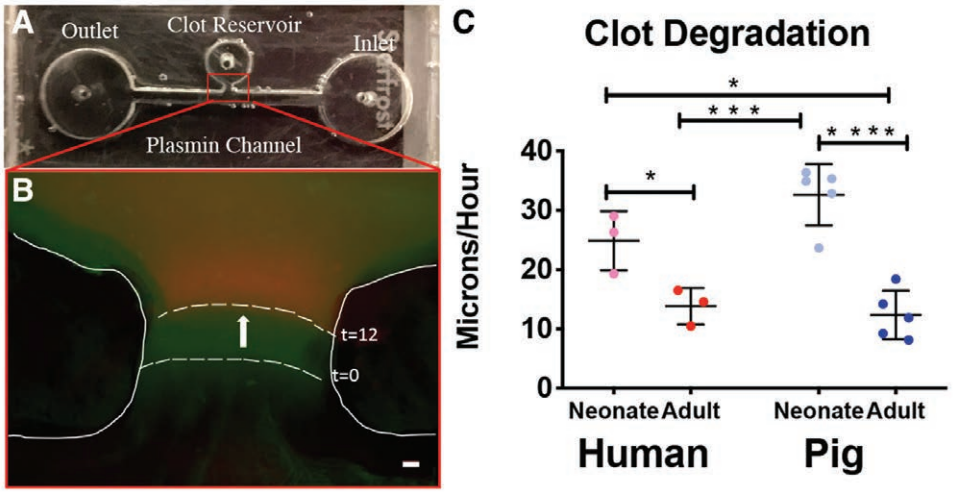

Fig. 6. Evaluation of plasma clot degradation with a custom microfluidic device. Top view of the device (*A*). Initial (*green*) and final (*red*) frames of clot boundary overlaid with false coloring (*B*). Average degradation rates ± SD. Neonatal humans, N = 3; adult humans, N = 3; neonatal pigs, N = 5; adult pigs, N = 5. Scale = 10 μm. **P* < 0.05, ***P* < 0.01, ****P* < 0.001, *****P* < 0.0001.

Analysis of Procoagulants in Porcine Model of Hemodilution

Neonatal porcine plasma was diluted to model the dilutional coagulopathy and associated reduction in fibrinogen seen after CPB.[7] Confocal microscopy was utilized to examine clot structure with or without the addition of factor VIIa, factor eight inhibitor bypassing activity, RiaSTAP, or platelet-like particles (fig. 7). Clots constructed of diluted porcine plasma were porous and heterogeneous in structure. The addition of all hemostatic therapies enhanced formation of the fibrin network with more complete fibrin matrices. The addition of platelet-like particles to diluted porcine plasma resulted in clots with statistically significant higher fiber density values (diluted plasma, 0.22 ± 0.17; factor VIIa, 0.31 ± 0.12; factor eight inhibitor bypassing activity, 0.61 ± 0.29; RiaSTAP, 0.57 ± 0.19; platelet-like particles, 0.83 ± 0.40; diluted *vs.* factor VIIa, $P = 0.989$; diluted *vs.* factor eight inhibitor bypassing activity, $P = 0.122$; diluted *vs.* RiaSTAP, $P = 0.199$; diluted *vs.* platelet-like particles, $P = 0.005$). Clot fiber alignment in the presence of factor VIIa was similar to control. The addition of factor eight inhibitor bypassing activity and platelet-like particles resulted in decreased, although not statically significant, alignment values (diluted plasma, 1.13 ± 0.09; factor VIIa, 1.16 ± 0.08; factor eight inhibitor bypassing activity, 1.06 ± 0.01; RiaSTAP, 1.02 ±0.10; platelet-like particles, 1.06 ± 0.01; diluted *vs.* factor VIIa, $P = 0.989$; diluted *vs.* factor eight inhibitor bypassing activity, $P = 0.340$; diluted *vs.* RiaSTAP, $P = 0.886$; diluted *vs.* platelet-like particles, $P = 0.402$). Next, clottability was determined for diluted neonatal plasma with and without the addition of procoagulants. Diluted neonatal porcine plasma clots had a lower average clottability (47 ± 31%) than those formed from factor VIIa (66 ± 24%; factor eight inhibitor bypassing activity, 79 ± 20%; RiaSTAP, 86 ± 6%; or platelet-like particles, 88 ± 8%; diluted *vs.* factor VIIa, $P = 0.225$; diluted *vs.* factor eight inhibitor bypassing activity, $P = 0.126$; diluted *vs.* RiaSTAP, $P = 0.039$; diluted *vs.* platelet-like particles, $P = 0.047$).

Discussion

Our results show that age-related differences identified in human fibrinogen are mirrored in pigs, thus confirming piglets as an appropriate preclinical model to evaluate the effects of neonatal specific hemostatic therapies on the fibrin network. To determine this, we thoroughly analyzed several aspects of fibrinogen and its resultant fibrin network across both species. We found that fibrinogen concentration and functionality in plasma collected from piglets accurately parallels those observed in plasma collected from human neonates. Fibrin network structure, when analyzed *via* confocal and cryogenic scanning electron microscopy, also displayed similar tendencies with highly aligned fibrin networks in both neonatal species compared to highly branched networks in adults. Lastly, we assessed fibrin network stiffness and degradation patterns between neonates and adults in both species and again found substantial similarities. To assess a potential application of post-CPB coagulopathy, we analyzed the structural and functional effects of several procoagulant therapies on the fibrin network formed from diluted piglet plasma. We found that the *ex vivo* addition of factor VII, factor eight inhibitor bypassing activity, RiaSTAP, and platelet-like particles augmented fibrin network properties as seen in our previous studies performed with human neonatal plasma obtained after CPB.[17,18]

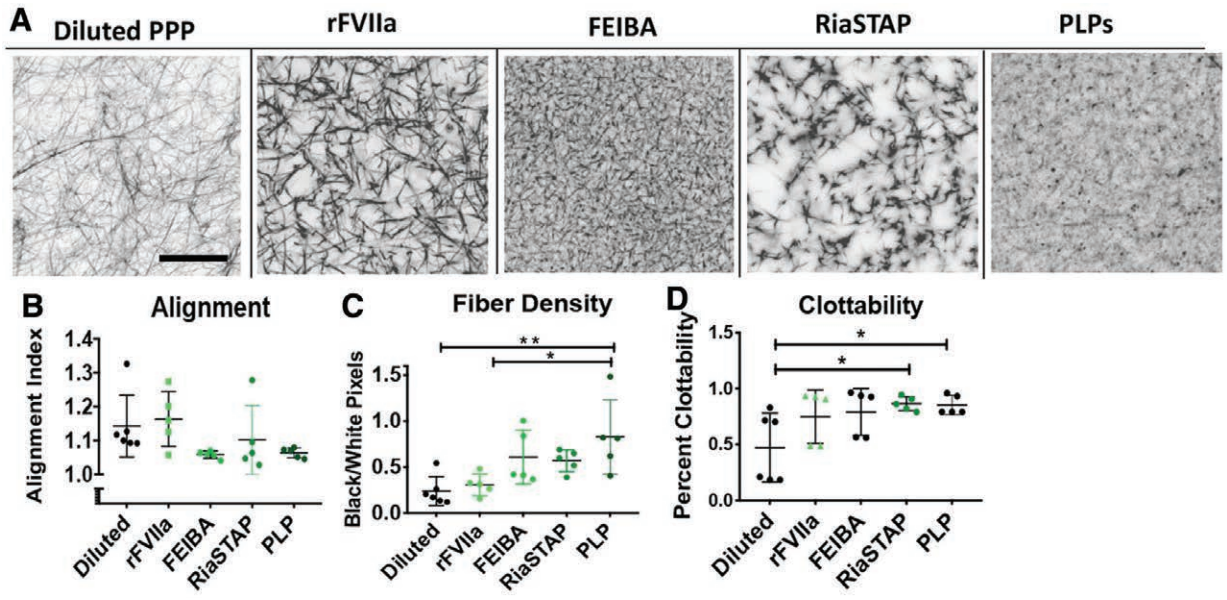

Fig. 7. Structural and functional analysis of hemostatic agents in diluted neonatal porcine plasma. (*A*)Representative images are shown of diluted neonatal porcine plasma in the absence or presence of factor eight inhibitor bypassing activity (FEIBA), factor VII (rFVIIa), or platelet-like particles (PLPs). Average clot fiber density (*B*), alignment (*C*), and clottability (*D*) are reported ± SD. Structural analysis: plasma, N = 7; FEIBA, factor VII, RiaSTAP, PLPs, N = 5. Clottability: platelet poor plasma, N = 6; FEIBA, factor VII, RiaSTAP, PLPs, N = 5. **P* < 0.05, ***P* < 0.01.

Coagulopathy can considerably complicate the clinical management of neonatal patients and results in significant morbidity and mortality.[4] It is frequently seen during major surgery, extracorporeal membrane oxygenation, and sepsis. When these patients require surgical treatment, anesthesiologists are presented with a challenging situation. Although our understanding of the importance of fibrinogen replacement in the treatment of severe bleeding has improved in recent years, available options to replenish it have not. The effectiveness of fresh frozen plasma to restore fibrinogen is poor due to a lack of potency, and the large volumes required in a neonate make it an impractical solution. Cryoprecipitate is more effective in providing higher concentrations of fibrinogen, but shares similar disadvantages to fresh frozen plasma: fibrinogen concentration is variable, blood group matching in neonates is recommended, time is required for thawing, and there is a risk of viral transmission. For those reasons cryoprecipitate is not available in several countries. Fibrinogen concentrate (RiaSTAP), made from pooled human plasma, is increasingly used to replete fibrinogen, but has limited availability and represents yet another form of adult fibrinogen that may not be compatible in the neonatal system.[4,7,24] Progress toward discovering improved methods to treat neonatal coagulopathy have been hindered by an inadequate understanding of the differences between adult and neonatal hemostasis, a limited number of well-performed clinical studies evaluating therapies to treat bleeding in neonates, and a lack of a validated animal model of neonatal coagulopathy. Our results represent a step toward this important goal.

To assess developmental similarities between human and porcine fibrinogen, we conducted a series of analyses comparing function, structure, and degradation among adult and neonatal human and porcine fibrin networks. To analyze the functionality of fibrinogen between species, we assessed clottability for all sample groups and found statistically significantly lower clottability values in human neonatal fibrinogen than were found in adult fibrinogen. This same relationship was reflected in the porcine samples. Structurally, we observed a three-dimensional, highly branched clot architecture in adult porcine samples *versus* thin, sheet-like fibrin matrices with little cross branching in neonatal porcine samples. Our quantitative analysis also revealed higher alignment and lower fiber density in neonatal porcine samples compared to adults. At a thrombin concentration of 0.5 U/ml, we performed a comparative image analysis with human samples and again identified similar structural differences between age groups in pigs and humans. Both neonatal species exhibited fibrin clots with a higher degree of alignment and statistically significant lower fiber densities when compared to corresponding adult clots. Moreover, these structural differences agree with our previous data examining fibrin clot structure constructed from neonatal and adult purified fibrinogen.[7] We speculate that these structural differences are the result of differences in fibrin polymerization. Future studies are necessary to elucidate the underlying mechanisms.

Our model validation also included analysis of human and porcine clot mechanical properties. Research has linked structurally dense, highly branched clots to greater clot stiffness.[25,26] Here, we used atomic force microscopy to measure plasma clot stiffness in both porcine and human samples. We found clots formed from neonatal human plasma had statistically significantly lower average stiffness values than those formed from adult human plasma ($P = 0.016$). These patterns were mirrored in clots formed from neonatal and adult porcine samples ($P = 0.015$).

In addition to polymerization rates, an accurate animal model must also display a fibrinolytic potential similar to humans. Thus, we measured degradation rates between age groups and species using a custom microfluidic device. We identified statistically significant faster plasma degradation rates in neonatal samples compared to adults. Previous research has indicated that fibrinolysis is related to clot structure, where denser, heavily branched clots have slower degradation rates than more porous clots.[27,28] Our data agrees with this relationship in that both neonatal porcine and human plasma clots exhibited rapid rates of degradation and lower fiber densities when compared to adult samples. This data is also consistent with our previous work where we identified statistically significant faster rates of fibrin clot degradation in neonates compared to adults, and when mixed together (to simulate transfusion with cryoprecipitate), clot degradation was statistically significantly slower than baseline neonatal rates.[7] We hypothesize that the intrinsic neonatal fibrinolytic system may not properly degrade adult fibrinogen, thus contributing to the high rate of thrombotic complications observed in neonates after cardiac surgery.[29] It is imperative that potential hemostatic therapies for surgical procedures be balanced to augment clotting while simultaneously limiting thrombotic complications. A valid preclinical animal model would aid this objective. Antifibrinolytic therapy is often used before, during, and after CPB to reduce bleeding by inhibiting degradation, but its clinical efficacy in the neonatal population is inconsistent.[30]

After validation of our model, we focused on its potential application as an *in vitro* model for post-CPB hemodilution. We diluted neonatal porcine plasma to mimic the reduction in clotting fibrinogen seen after CPB. Structural analysis of these samples revealed very porous clot architecture with low clottability (fig. 7), and emulated our previous experiments characterizing post-CPB clots made from neonatal plasma.[7,18] Next, to explore possible treatment options for post-CPB bleeding, novel and commercially available hemostatic therapeutics were applied to the diluted samples. Structurally, all therapeutics enhanced fibrin clot formation and resulted in more complete fibrin matrices. Furthermore, the addition of synthetic platelet-like particles to diluted plasma produced a statistically significant increase in fiber density. Again, the results from these structural analyses are in line with our previous studies demonstrating that the *ex vivo* addition of factor VIIa, factor eight inhibitor bypassing activity, RiaSTAP, and platelet-like particles to post-CPB human neonatal plasma augment fibrin network properties.[17,18] Future studies should include a thorough analysis of degradation rates within the neonatal system.

This study has several limitations. First, our experiments are conducted *ex vivo* with either purified fibrinogen or plasma and therefore may not accurately represent *in vivo* physiology. Specifically, our experiments did not account for the complexity of whole blood, including the crucial role of platelets in hemostasis. Future studies using whole blood samples and/or platelet-rich plasma are essential to better investigate the intricacy of *in vivo* coagulation and fibrinolytic responses. However, the simplified system utilized in our study allowed for the detailed focus on age-dependent differences in fibrinogen and plasma fibrin networks between humans and pigs. Also, due to the accelerated timeline of aging in pigs compared to humans, it is likely that the 8-week-old piglets used in this study do not accurately reflect the neonatal period in humans. The samples utilized in this study were obtained based on availability from North Carolina State University's School of Veterinary Medicine. Follow-up studies should include an analysis of younger porcine plasma samples to allow for more precise age matching between species. Nonetheless, we show that 8-week-old piglets could serve as a useful preclinical model for human neonatal fibrin deficiencies. Also, using 8-week-old piglets is logistically easier than very young, newborn pigs, as they are already weaned. Additionally, all sample groups utilized in this study included both male and female samples except for the adult porcine group in which there were only females. The experiments in this study have not been explored on the basis of sex and therefore it is possible that the addition of male pigs in the adult porcine group may alter results. This study utilized plasma samples from healthy piglets in order to establish a baseline *in vitro* model. However, the presence of congenital heart defects may add complexity to the coagulation system from poor circulation and cyanosis. Some porcine models of severe congenital heart disease, including tetralogy of Fallot, have been described.[31] In future research, porcine models with congenital heart defects should be used for *in vitro* characterization of plasma samples and *in vivo* analysis of bleeding to identify potential discrepancies between neonatal piglets without cardiac disease and piglets with complex congenital heart disease. Finally, the coagulopathy that results from CPB in neonates is complex and involves consumptive processes as well. Here, we concentrated only on the hemodilutional aspect of bypass-induced coagulopathy. However, focusing on the reduction in fibrinogen allowed us to examine the effect of procoagulants on fibrin properties in a less complicated system. While informative, future studies should expose neonatal piglets to CPB and subsequently characterize clotting properties.

In summary, our results validate that piglets can serve as an appropriate animal model capable of reflecting the developmental nuances observed in human fibrinogen. Recent evidence confirms that neonatal fibrinogen is qualitatively distinct from adult fibrinogen resulting in differences between neonatal and adult fibrin clot structure. In our analyses, we observed similar fibrinogen concentrations and clottability across species as well as similar age-related patterns in structure, mechanical, and degradation properties of adult and neonatal porcine and human samples. Based on these results we conclude that piglets are indeed an appropriate preclinical animal model for neonatal hemostasis. In addition, we demonstrated the feasibility of an *in vitro* model application through the analysis of several hemostatic therapies applied to diluted neonatal porcine plasma.

Acknowledgments

The authors would like to thank Eva Johannes, Ph.D., Director at the Cellular and Molecular Imaging Facility at North Carolina State University, Raleigh, North Carolina and Elaine Zhou, Ph.D., Research and Development Manager of the Surface Science Lab at the Analytical Instrumentation Facility at North Carolina State University, Raleigh, North Carolina, for technical assistance with microscopy.

Research Support

Supported by grant Nos. 16SDG29870005 from the American Heart Association (Dallas, Texas), DMR-1847488 from the National Science Foundation (Alexandria, Virgina), CDMRP W81XWH-15-1-0485 from the U.S. Department of Defense (Washington, D.C.), and R01HL130918-01A1 from the National Institutes of Health (Bethesda, Maryland).

Competing Interests

The authors declare no competing interests.

Correspondence

Address correspondence to Dr. Brown: Biomedical Partnership Center Building, 1001 William Moore Drive, Office 26, Raleigh, North Carolina 27606. aecarso2@ncsu.edu. Information on purchasing reprints may be found at www.anesthesiology.org or on the masthead page at the beginning of this issue. ANESTHESIOLOGY's articles are made freely accessible to all readers, for personal use only, 6 months from the cover date of the issue.

References

1. Andrew M, Paes B, Milner R, Johnston M, Mitchell L, Tollefsen DM, Castle V, Powers P: Development of the human coagulation system in the healthy premature infant. Blood 1988; 72:1651–7
2. Ignjatovic V, Mertyn E, Monagle P: The coagulation system in children: Developmental and pathophysiological considerations. Semin Thromb Hemost 2011; 37:723–9
3. Toulon P: Developmental hemostasis: Laboratory and clinical implications. Int J Lab Hematol 2016; 38 Suppl 1:66–77
4. Guzzetta NA, Allen NN, Wilson EC, Foster GS, Ehrlich AC, Miller BE: Excessive postoperative bleeding and outcomes in neonates undergoing cardiopulmonary bypass. Anesth Analg 2015; 120:405–10
5. Guzzetta NA: Benefits and risks of red blood cell transfusion in pediatric patients undergoing cardiac surgery. Paediatr Anaesth 2011; 21:504–11
6. Guzzetta NA, Williams GD: Current use of factor concentrates in pediatric cardiac anesthesia. Paediatr Anaesth 2017; 27:678–87
7. Brown AC, Hannan RT, Timmins LH, Fernandez JD, Barker TH, Guzzetta NA: Fibrin network changes in neonates after cardiopulmonary bypass. ANESTHESIOLOGY 2016; 124:1021–31
8. Ignjatovic V, Lai C, Summerhayes R, Mathesius U, Tawfilis S, Perugini MA, Monagle P: Age-related differences in plasma proteins: How plasma proteins change from neonates to adults. PLoS One 2011; 6:e17213
9. Ignjatovic V, Ilhan A, Monagle P: Evidence for age-related differences in human fibrinogen. Blood Coagul Fibrinolysis 2011; 22:110–7
10. Münster AM, Olsen AK, Bladbjerg EM: Usefulness of human coagulation and fibrinolysis assays in domestic pigs. Comp Med 2002; 52:39–43
11. Olsen KA, Hansen AK, Jespersen J, Markmann P, Bladbjerg EM: The pig as a model in blood coagulation and fibrinolysis research. Scand J Lab Anim Sci 1999; 26:214–25
12. Zentai C, Braunschweig T, Rossaint R, Daniels M, Czaplik M, Tolba R, Grottke O: Fibrin patch in a pig model with blunt liver injury under severe hypothermia. J Surg Res 2014; 187:616–24
13. Inaba K, Barmparas G, Rhee P, Branco BC, Fitzpatrick M, Okoye OT, Demetriades D: Dried platelets in a swine model of liver injury. Shock 2014; 41:429–34
14. Greek R, Rice MJ: Animal models and conserved processes. Theor Biol Med Model 2012; 9:40
15. Zeng L, Choonara I, Zhang L, Li Y, Shi J: Effectiveness of prothrombin complex concentrate (PCC) in neonates and infants with bleeding or risk of bleeding: A systematic review and meta-analysis. Eur J Pediatr 2017; 176:581–9
16. Hedner U, Erhardtsen E: Potential role for rFVIIa in transfusion medicine. Transfusion 2002; 42:114–24
17. Brown AC, Stabenfeldt SE, Ahn B, Hannan RT, Dhada KS, Herman ES, Stefanelli V, Guzzetta N, Alexeev A, Lam WA, Lyon LA, Barker TH: Ultrasoft microgels displaying emergent platelet-like behaviours. Nat Mater 2014; 13:1108–14

18. Nellenbach K, Guzzetta NA, Brown AC: Analysis of the structural and mechanical effects of procoagulant agents on neonatal fibrin networks following cardiopulmonary bypass. J Thromb Haemost 2018; 16:2159–67
19. Nandi S, Sproul EP, Nellenbach K, Erb M, Gaffney L, Freytes DO, Brown AC: Platelet-like particles dynamically stiffen fibrin matrices and improve wound healing outcomes. Biomater Sci 2019; 7:669–82
20. Nandi S, Brown AC: Platelet-mimetic strategies for modulating the wound environment and inflammatory responses. Exp Biol Med (Maywood) 2016; 241:1138–48
21. Sproul E, Hannan R, Brown AC: Characterization of fibrin-based constructs for tissue engineering, Methods in Molecular Biology-Biomaterials. New York, Springer, 2018
22. Timmins LH, Wu Q, Yeh AT, Moore JE Jr, Greenwald SE: Structural inhomogeneity and fiber orientation in the inner arterial media. Am J Physiol Heart Circ Physiol 2010; 298:H1537–45
23. Spiess BD, Armour S, Horrow JC, Kaplan JA, Koch C, Karkouti K, Body SC: Transfusion medicine and coagulation disorders, Kaplan's Essentials of Cardiac Anesthesia, 2nd edition. Edited by Kaplan JA. Philadelphia, Elsevier, 2018, pp 685–714
24. Williams GD, Bratton SL, Ramamoorthy C: Factors associated with blood loss and blood product transfusions: A multivariate analysis in children after open-heart surgery. Anesth Analg 1999; 89:57–64
25. Undas A, Ariëns RA: Fibrin clot structure and function: A role in the pathophysiology of arterial and venous thromboembolic diseases. Arterioscler Thromb Vasc Biol 2011; 31:e88–99
26. Weisel JW: Structure of fibrin: impact on clot stability: Structure of fibrin: impact on clot stability. J Thromb Haemost 2007; 5:116–24
27. Weisel JW, Litvinov RI: The biochemical and physical process of fibrinolysis and effects of clot structure and stability on the lysis rate. Cardiovasc Hematol Agents Med Chem 2008; 6:161–80
28. Undas A: Prothrombotic fibrin clot phenotype in patients with deep vein thrombosis and pulmonary embolism: A new risk factor for recurrence. Biomed Res Int 2017; 2017:8196256
29. Manlhiot C, Menjak IB, Brandão LR, Gruenwald CE, Schwartz SM, Sivarajan VB, Yoon H, Maratta R, Carew CL, McMullen JA, Clarizia NA, Holtby HM, Williams S, Caldarone CA, Van Arsdell GS, Chan AK, McCrindle BW: Risk, clinical features, and outcomes of thrombosis associated with pediatric cardiac surgery. Circulation 2011; 124:1511–9
30. Androupoulus DB, Stayer SA, Mossad EB, Miller-Hance WC: Anesthesia for Congenital Heart Disease, 3rd edition. Hoboken, New Jersey, Wiley-Blackwell, 2015
31. Camacho P, Fan H, Liu Z, He J-Q: Large mammalian animal models of heart disease. J Cardiovasc Dev Dis 2016; 3:30